
ORTHOGAN:HIGH-PRECISION IMAGE GENERATION FOR TEETH ORTHODONTIC VISUALIZATION

Shen Feihong
Jilin University
gregoryfeihong@gmail.com

Liu jingjing
Zhejiang University
12221107@zju.edu.cn

Li Haizhen
Shanghai Jiao Tong University School of Medicine
569286671@qq.com

Zheng Youyi
Zhejiang University
youyizheng@zju.edu.cn

ABSTRACT

Patients take care of what their teeth will be like after the orthodontics. Orthodontists usually describe the expectation movement based on the original smile images, which is unconvincing. The growth of deep-learning generative models change this situation. It can visualize the outcome of orthodontic treatment and help patients foresee their future teeth and facial appearance. While previous studies mainly focus on 2D or 3D virtual treatment outcome (VTO) at a profile level, the problem of simulating treatment outcome at a frontal facial image is poorly explored. In this paper, we build an efficient and accurate system for simulating virtual teeth alignment effects in a frontal facial image. Our system takes a frontal face image of a patient with visible malpositioned teeth and the patient's 3D scanned teeth model as input, and progressively generates the visual results of the patient's teeth given the specific orthodontics planning steps from the doctor (i.e., the specification of translations and rotations of individual tooth). We design a multi-modal encoder-decoder based generative model to synthesize identity-preserving frontal facial images with aligned teeth. In addition, the original image color information is used to optimize the orthodontic outcomes, making the results more natural. We conduct extensive qualitative and clinical experiments and also a pilot study to validate our method.

Keywords Deep Learning, Computer simulation, teeth alignment

1 Introduction

Many parts of clinical treatment plan design can be time-consuming and redundant. In recent years, deep learning models have been developed to help doctors get rid of some data processing work. Numerous deep learning integrated software have been developed to analyze and visualize an orthodontic effect, such as Quick Ceph Image [1] and Dolphin Imaging [2]. In the meantime, smile simulation of the frontal face is getting more and more attention [3, 4]. Smile simulation has the ability to attract people to do orthodontic treatment. It is rational that patients who choose invisible teeth alignment have the willing to know what their frontal facial images look like in different treatment stages. However, apart from its advertising effect, it is still a serious digital medical technology. Orthodontists and patients who can quantitatively assess their per-step treatments may wish to communicate about the treatment based on the simulation and make the adjustment in time. That's being said, the generated teeth images should be strictly aligned with the patient's actual teeth and have the real outlooks simultaneously. Nevertheless, due to the complicated data formation in this task, the previous works either fail to efficiently generate an aligned frontal smile image with high quality or the results do not convey the accurate virtual outlooks. Therefore, an accurate and efficient system that can automatically predict high-quality smile simulation in photographs is needed for orthodontic visualization.

Even if the orthodontists can not directly draw some 2D teeth images by their professional knowledge and tell the patients that these images are the expected shapes of your teeth under current treatment schedule, they can still provide

reliable information including the 3D teeth models and their planning prescriptions (i.e., how individual tooth moves at each orthodontic stage). Then a natural goal of our system is replacing the teeth region of the face images with the image generated by these 3D teeth models. Here we got data from two different modalities: 3D teeth model and RGB image. In the real clinic application, we can not directly cast the 3D data into the deep model because of its large consumption of resource (both time resource and memory resource). In this work, we firstly transfer the 3D data to other modalities, including depth image, sketch image, and label mask. Our work focuses on how to efficiently transfer these modalities and make good use of them to generate the high quality frontal face images that include a big, charming smile.

The most essential part of this task is image generation. In this work, we choose the generation adversarial network (GAN) as our deep generation model. In last decade, generative adversarial network (GAN) [5, 6, 7] have been utilized in many real world applications and have achieved state-of-art performances. Many architectures of the GAN have been proposed to improve the fidelity and diversity of the generated signal including WGAN [8], BigGAN [7] *et al.*. In recent years, StyleGAN [9] has been known for its ability to generate realistic images in various domains. EditGAN [10] applied it to generate realistic facial images, which allow users to edit images by modifying highly detailed part segmentation masks. Inspired by the success of multi-modal GAN [11], we present Orthodontic Generative Adversarial Network (OrthoGAN), which combine the teeth geometry information from the 3D model and teeth visual characteristics from the RGB image to generate the corresponding after-treatment smile face photograph. Specifically, the Unet-liked architecture in the network structure enables the GAN to fitting the slight edge of teeth in the input map and the style-based architecture in the network allows the GAN to simulate complicated illumination condition on the faces of the teeth. We will also discuss how to process different modalities before and after the generation to achieve better performance.

As we said before, the 3D teeth model needed to be transferred into other modalities. Although the dentists provide us the mediate 3D teeth object, directly casting encoding feature of these objects into the network is over laconic and makes it hard for the network to converge. Following previous work [3], we take the 2D images as the input of our GAN. Different from previous work, which took expectation maximization (EM) algorithm to project the 3D teeth objects, in this work we take advantage of the developed differentiable rendering technique which takes less time assumption and achieves better projecting accuracy.

Our contributions of this work can be summarized as follows:

- We propose a new system which takes the modified inner mouth scanned model and the frontal smile face image as input and generate same face image with different teeth appearance aligned with modified 3D teeth model.
- Our method leverages differential rendering and surpasses the performance of traditional method in teeth pose fitting.
- To the best of our knowledge, we are the first to use multi-modal conditional style-based GAN in the oral domain and achieve great sample quality. Some of the innovations of our network can be used on other general generation tasks.

2 Materials and Methods

2.1 data description

We get two modal data at first: a face photograph of a patient with visible misaligned teeth X and a list of 3D objects representing the changing of patient’s teeth during the alignment. Let us denote the object in list by T_i , where $i \in [0, N]$ indexes stage. The corresponding generated face image is \hat{X}_i , where $i \in [1, N]$ since the first 3D object T_0 directly corresponds to X .

We select the frontal face data from several open-source human face datasets, including Flickr-Faces-HQ, CelebA *et al.*. We cut the squared mouth region of the images and resize them to 256×256 resolutions. We manually labeled part of the selected data for the training of our instance and semantic segmentation networks. Then we leveraged the trained networks labeling the rest of the dataset. As shown in Figure 1, the entire dataset contained 12000 mouth images with their teeth silhouettes, teeth masks and mouth labels which are used to train our OrthoGAN with uniform image size. The 3D teeth models are constituted by the initial teeth model T_0 and its target align teeth models T_i scheduled by orthodontists. They share the same local coordinate system, which means we can render them through the same camera parameters.

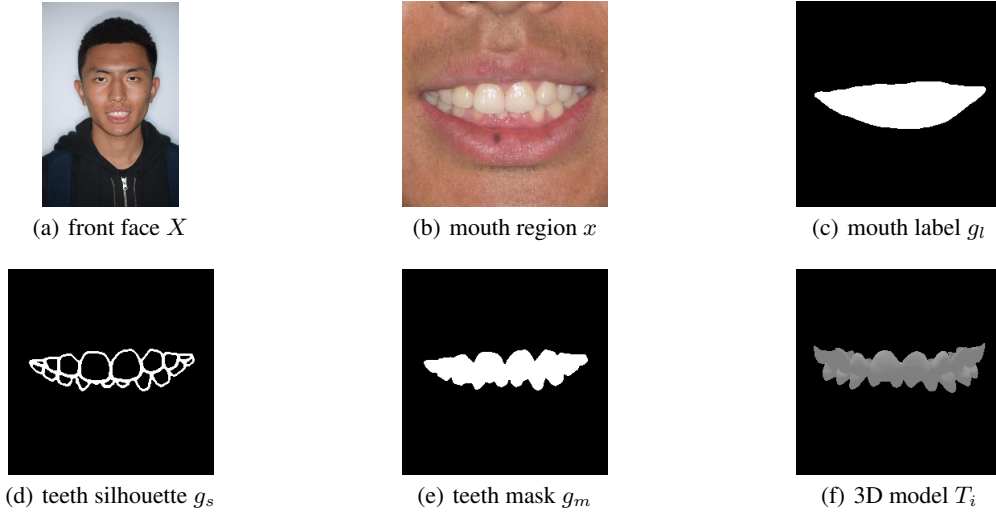


Figure 1: one sampled case with some different data formats we used in this work

Following the previous work [3], we mainly process the mouth region image. Firstly, we leverage a trained face instance segmentation network to get the square image x of mouth region from X . We take yoloV5 as the architecture of our network. The relative position of x to X is saved in system buffer for the post-process operation in the final stage. Then we train a multi-head semantic segmentation network which take x as input and output the teeth silhouette g_s and in-mouth region g_l of teeth in image under the supervise of labeled data (an example of g_s and g_l is shown in Figure 1). This network are designed based on UNet [12] whose latest extensions like UNet++ [13], 3D UNet [14] and TransUNet [15] have been the leading medical image segmentation methods. We will discuss the detail of these networks in the experimental setup section.

Our system mainly includes four stages to process the data. In the first stage, we apply two segmentation networks on X to get the x and its corresponding g_m , g_l and g_s . In the second stage, we prepare the input data of our OrthoGAN, leveraging silhouette images in the first stage and the 3D objects T_i through differential rendering. In the third stage, our deep model OrthoGAN generates the aligned teeth image corresponding to the 3D object in the former stage. In the last stage, we apply some post-process on the generated image \hat{x} and put it back to the frontal face image X . The overall framework of our system is illustrated in Figure 2(a).

2.2 modal transfer

Different from previous work [3], we use differential rendering to make our system more accurate and robust on transferring the data modal. Given the teeth silhouette g_s of the image x and the teeth model T_0 at start, our goal is reconstructing the parameters θ of the camera when X got shot and apply it on our rendering model. Then our renderer r_θ can project T_0 to \hat{g}_s closer to g_s in the region of g_l (Figure 2(a)). Thanks to the differentiability of the renderer, we can set the initial parameters and iteratively optimize them under the guidance of a loss function till fitting. In this work, we simply choose l_2 -norm as our loss function:

$$L_\theta := \|g_l * g_s - g_l * r_\theta(T_0)\|_2^2 \quad (1)$$

The optimized parameter θ of our rendering model includes camera focal length, translation and rotation matrix of camera in global coordinate system, offset of lower teeth towards upper teeth. Once L_θ is lower than a threshold, which means that the parameters are close enough to the real situation. We apply these parameters on other 3D object then get the silhouettes g_s of every 3D object in following stages. Every g_s keep consistent with each other and has the correct relative position to the frontal face image.

Popular renderers can not directly render the special silhouette of the 3D object. The common renderer usually includes one rasterizer and one shader, while our renderer has two shaders, both are customized. The first one shade the teeth object separately based on its teeth number. We can get every single tooth's edge and add them together to get the silhouette of the whole teeth. The second shade the color of our 3D teeth based on the distance between the teeth faces and our camera. Start from white color, the longer the distance is, the darker the color is. Through this shader, our renderer can get the depth image of the 3D object. However, not all teeth can be seen in the frontal face image because

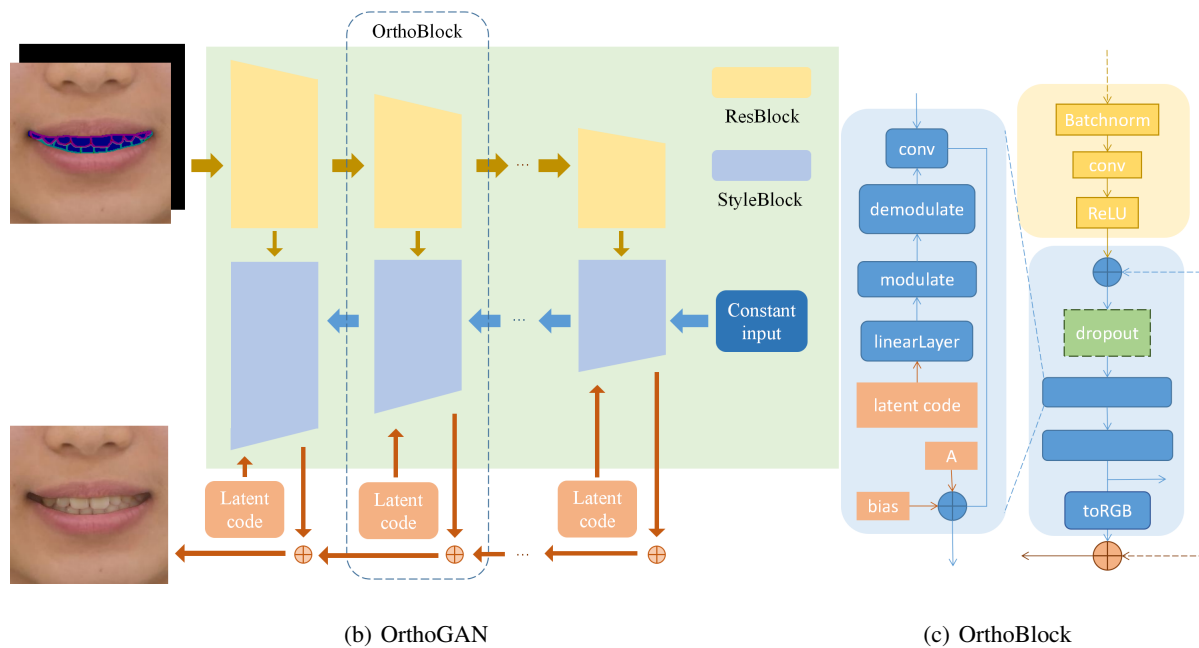
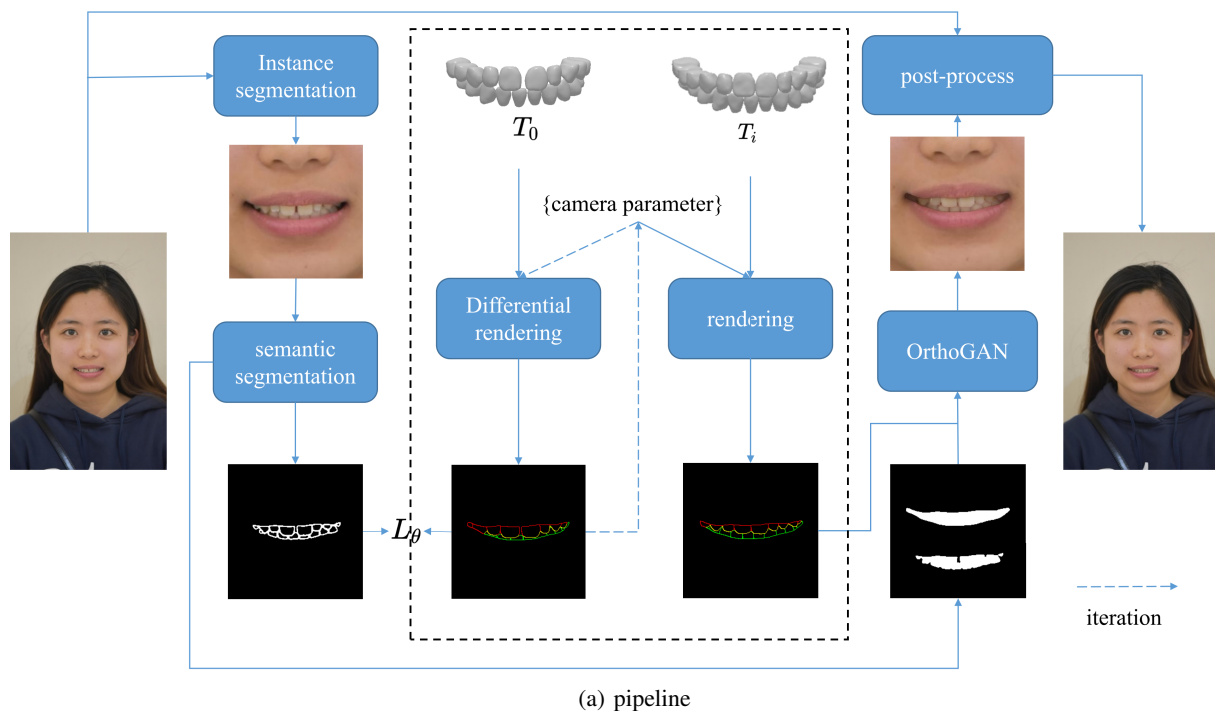


Figure 2: **High-level system overview.** (a) The pipeline of our approach in the inference stage. Dashed box denotes the 3D registration optimization directed by the loss function L_θ . (b) The architecture of our OrthoGAN. The ResBlock and part of the StyleBlock constitute a UNet-like structure. The rest part of the StyleBlock is based on the style generation structure. Together, they formed an OrthoBlock. The final image is the sum of the up-sampled output of each OrthoBlock. (c) The inner structure of StyleBlock. A denotes a broadcast and scaling operation. The dropout layer aims to circumvent over fitting in training stage and is removed in inference stage.

of the special physical condition of human oral cavity. So we ignore some teeth whose distances are bigger than a threshold. These two shaders share the same parameters so once the silhouette is fitted, the depth image is in correct position. Setting the non-zero elements in depth image as one, we get the teeth mask g_m of the 3D model. The former work [3] does not contain the modality of depth map, while we found that without this modality, the GAN is easily to muddle the existence of the teeth. Moreover, in previous work, the silhouette is directly cast into the generator. While in this work, we remove the part of g_m and g_s outside the region g_l . We found that this process can significantly improve the quality of the generated image on the edge of g_l .

2.3 OrthoGAN

After semantic segmentation and differentiable rendering, we get the mouth region g_l , the teeth silhouette g_s and teeth masks g_m of target generated 2D teeth \hat{X}_i corresponding to the 3D teeth model T_i . The goal of our OrthoGAN is to project these parameters to generate the teeth image \hat{x}_i aligned with T_i inside the mouth region g_l .

$$\begin{aligned}\hat{x}_i &= \text{OrthoGAN}(g_l, g_s, g_m, x_0) \\ x_0(1 - g_l) &= \hat{x}_i(1 - g_l)\end{aligned}\quad (2)$$

The reason we do not concatenate the 3D model rendered image and the human face is the complexity of oral environment and teeth material which make realistic rendering difficult. Meanwhile, the GANs have been proved to be able to capture these two characteristics [7]. As in 2, our task turns to conditional generation after modal transfer and there are numerous style-based conditional GANs, we choose StyleGAN [9] as the architecture of our generation model.

PixelStylepixel (pSp) [16] is a classical StyleGAN inversion architecture. It seems like our OrthoGAN can take a similar encoder-decoder design whose decoder D_{ortho} is a trained teeth generator of StyleGAN which take the output of the encoder E_{ortho} as input.

$$\hat{x}_i = D_{ortho}(E_{ortho}(g_l, g_s, g_m, x_0))\quad (3)$$

However, we found that this method can't reconstruct the correct shape of teeth even if we specially designed a shape training loss to supervise the generation. And this can be explained by information theory (Figure 4(b)). The information of teeth shape is partly lost during the encoding process. In fact, the previous GAN inversion tasks [17, 18] about human face always fail to reconstruct the teeth edge. To overcome this problem, we insert a special UNet architecture into our OrthoGAN to guide the generation. As show in Figure 2(c), the yellow layers extract the hierarchical geometry features of input and add them on the corresponding mid hidden feature in the blue style architecture. The mid hidden feature can be considered as a high dimensional image information that can be translate to an RGB image in the toRGB layer. When we add the geometry feature maps to the mid hidden feature, we actually give the outline guidance of target teeth image generation.

To keep the spatial attribution of g_s and g_m , we cascade some simple Resnet blocks [19] to extract the features. It makes our encoder averagely 10 times smaller than previous styleGAN encoder in parameter size. The large scale of conventional encoder can be attributed to the fact that teeth object often contain imperceptible details which require repeated functional evaluation in the W+ space of styleGAN [20]. While our UNet architecture can directly provide the high frequency features to the generator so our model also converges faster than common style-based inversion models. Compared to the previous work [3] which directly takes a UNet as their generator, the style architecture in our generator performs better in reconstructing the illumination effect on teeth while keeping the teeth shape correct (Figure 3).

In Equation 2, the region outside the mouth in \hat{x}_i is expected to keep aligned with x_0 . It is also a general problem in image editing field: when we edit part of an image, we want the generated image to keep the rest part untouched. Since the \hat{x}_i will be put back to X_i , there will be an obvious color gap on the face if we do not handle this problem properly. The non-square shape of g_l makes it impossible for the generator to only generate teeth part image without influencing the mouth region. Rather than using poisson blending in previous work [4], we append a fusion layer on the end of the network. Labeling the region outside of mouth as $1 - g_l$ as in Equation 2, this layer replace the region $1 - g_l$ of \hat{x}_i with x_0 .

$$\hat{x}_i = \hat{x}_i \odot g_l + x_0 \odot (1 - g_l)\quad (4)$$

At the beginning of the training stage of OrthoGAN, the generated image exhibit discord on the edge of g_l . Then the discriminator force the generator learn the edge through our encoder and generate harmony interspace. In other word, the process of learning to generate harmony mouth edge teeth image based on g_l has been integrated in the classical GAN loss [21]. In the end, the generator can generate natural teeth image while keep the region $1 - g_l$ the same as x_0 . This method is similar to another recent work [22] but our network does not need the resample operation because of our ResBlock (Figure 2(b)).

In our OrthoGAN, the shape of teeth is dependent on spatial features from UNet architecture. To increasing the interpretive of our architecture, in the inference stage, we take the constant latent codes in W+ space to represent

	Ortho	TSyn	pSp	P
Simulation authenticity	9.05±0.64	8.03±0.36	7.12±0.45	0.000
Simulation aesthetics	7.97±0.65	8.06±0.58	6.83±0.38	0.000
Image quality	7.74±0.38	7.99±0.34	6.88±0.38	0.000
<u>Simulation authenticity</u>	7.95±0.37	8.03±0.36	6.91±0.45	0.000**
<u>Simulation aesthetics</u>	7.71±0.44	7.88±0.38	6.90±0.40	0.000**
<u>Image quality</u>	7.71±0.40	7.79±0.42	6.96±0.36	0.000**

Table 1: The scores statistics to the simulation results of the three models. The underlined ones are the orthodontists’ score, and the unlined ones are the patients’ scores. *** : $p < 0.001$; ** : $p < 0.01$; * : $p < 0.05$.

the material and illumination of teeth. We take the average latent code in training stage as the constant term of our OrthoGAN. This strategy help us generate teeth with unified texture and mitigate the parameter size of our model because we do not need an additional StyleGAN encoder to generate the latent code.

2.4 Post-Progress

In order to make the generated result more realistic, we use the orthogonalization of the color space to correct the OrthoGAN-generated tooth color by the original tooth color, which is based on mean and standard deviation [23]. It is worth noting that only the color is changed, and other properties of the image will not be affected.

There is little correlation between the axes in Reinhard [24]’s perception-based color space $l\alpha\beta$. First we convert the image from RGB space to $l\alpha\beta$ space. Then the mean and variance of the output image are transformed to the mean and variance of the original image. Finally, convert the result back to RGB space and get an image closer to the original tooth color.

2.5 Experimental Setup and Evaluation

All deep networks in this work use Adam optimizer with different learning rates: 0.0001 for segmentation networks, 0.001 for differential rendering and 0.00005 for OrthoGAN. The discriminator architecture and training losses of OrthoGAN is same to StyleGAN2 [25]. It takes 5 minutes to train segmentation networks, 48 hours to train OrthoGAN and 1 minute to optimize differential rendering with 1000 iterations. All experiments are running on a server with eight Nvidia 3090 GPUs, an AMD EPYC 7402 24-Core processor, and 252 GB RAM.

Our evaluation mainly contains two aspects: 3D model position fitting and teeth image generation. We compare fitting accuracy with the EM algorithm of iOrthoPredictor [3] by the \mathcal{L}_{fit} which indicates the difference between the target teeth silhouette and the predicted teeth silhouette. However, sometimes lower difference do not represent the camera of the render is well posed, so we hired 20 orthodontists to judge whether our generated teeth images are aligned with the 3D teeth models. Typically, too closer camera in z axis make the generated teeth in image bigger than origin teeth and the wrong y axis position of camera makes the deviation of generated teeth (Figure 4(c)).

We train pixelStylepixel [16], TSynNet of iOrthoPredictor [3] and our OrthoGAN with same training dataset. The training parameters of other two networks follow their original paper. We apply the segmentation network S on the generated image \hat{x}_i of these three networks to generate the teeth silhouettes \hat{g}_s . The metric \mathcal{L}_{gen} is proposed to quantitatively evaluate the difference between \hat{g}_s and g_s . To further evaluate the quality of our generated images, we conducted a user study with 80 participants, consisting of 60 ordinary people in the age range of 20-30 (a majority of them were college students) and 20 orthodontists with over 5 years of experience. The participants were required to score the synthesized images on different dimensions. Ordinary people rate the aesthetics of the results, while orthodontists, due to their expertise, mainly evaluate whether our result conform to medical rules. The score range was from 0 to 10.

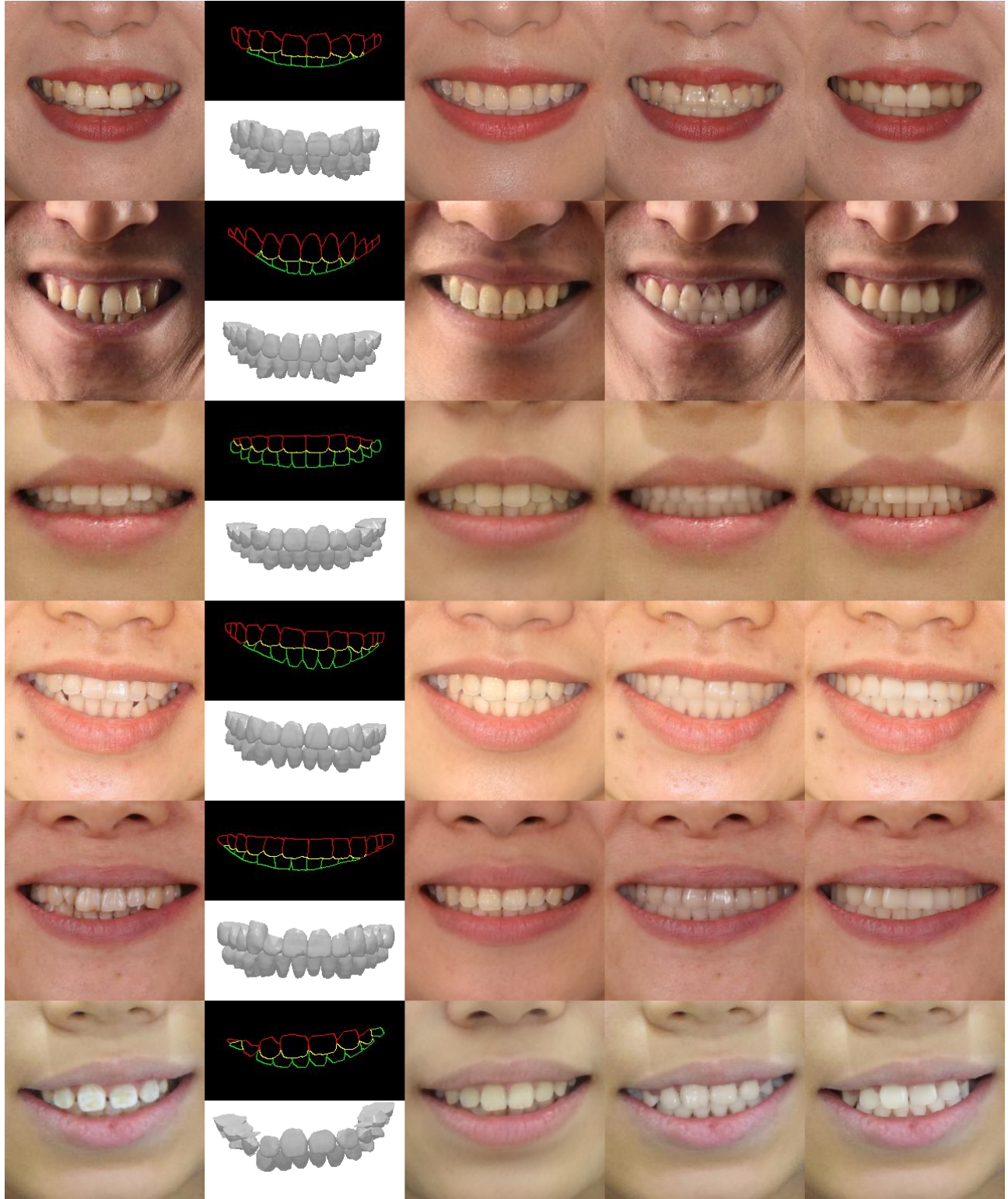
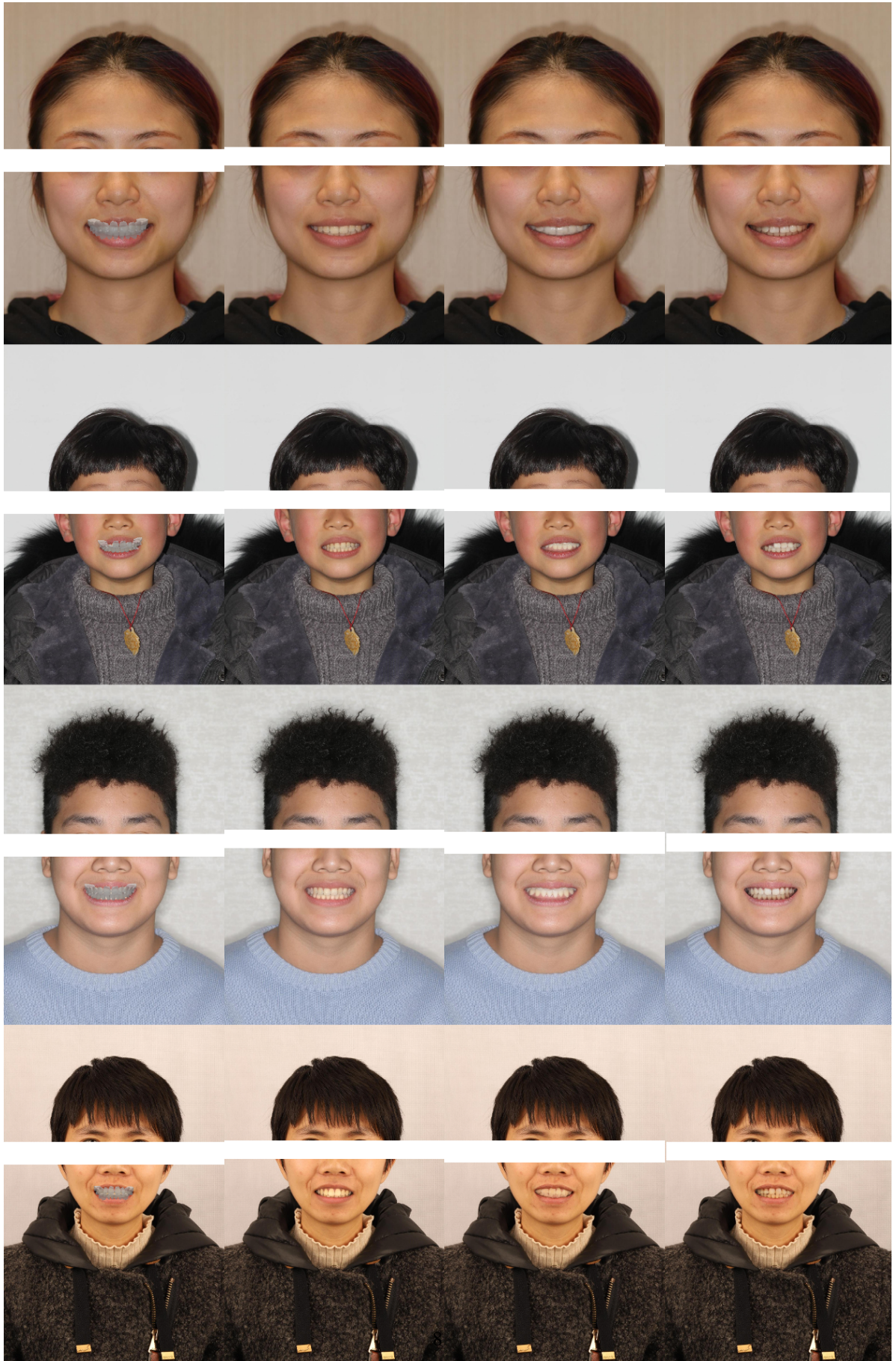


Figure 3: Generation quality comparison on teeth alignment cases. For each row, from left to right are the origin mouth images, the target silhouette of teeth, the teeth image generated by pSp, the teeth image generated by TSynNet, the teeth image generated by OrthoGAN. It is clear that our result align with the target silhouettes better and successfully reconstruct the original material of teeth.



(a) 3D model

(b) pSp using DF

(c) TSynNet using EM algo-

(d) OrthoGAN using DF

3 Results

In this section, we show the results of our approach and iOrthoPredictor on a variety of orthodontic cases with teeth in diverse shapes, appearance, and arrangements. It is noteworthy that all the results presented in this paper, except explicitly indicated, are generated without any user intervention.

Similar to iOrthoPredictor, in our system, the time consumption of generation model and segmentation model is negligible. What really influence the experience of using is the duration of the pose fitting stage. The detection of silhouette maps and mouth cavity mask by the segmentation networks takes 6ms per image. While the previous work takes 2 seconds for 30 optimization iterations [3], our method which utilize differential rendering averagely takes 1.8 seconds for 100 iterations. In some cases, the optimizing process reaches low \mathcal{L}_{fit} quickly and takes less than 100 iterations.

As we mentioned before, the precision of the pose fitting can be evaluated by the movement and scaling of the teeth edge as shown in Figure 4(a). In the 263 cases of our experiment, the pose fitting algorithm of previous work make obvious movement mistake like Figure 4(a) row 2 and 3 of TSynNet in 30 cases and fail to keep the consistent of the teeth size like Figure 4(a) row 1 of TSynNet in 201 cases. Meanwhile, our differential rendering method occurs the movement mistake in only 10 cases and wrongly scales the teeth size in 40 cases.

Since the RGB image of the frontal face is the final data modality that the dentists and patients received, the core standard to evaluate the system is definitely the ability of our generation model which is OrthoGAN in our system. Here we show the high quality after-orthodontics mouth image generated by our OrthoGAN in Figure 3 and Figure 4(d). We also list the result of other generation model from the same treatment to do the comparison. The pSp [16] model is clearly unable to reconstruct the geometry of the teeth shape. Some of the result of TSynNet have the black spots on the surface of the teeth. In the most cases OrthoGAN handles the lip edge part of the teeth better than TSynNet and so does the mouth corner part: the shadow of teeth in the corner appears to be unnatural in some cases.

To quantify the modal reconstruction ability of the generation model, we apply the segmentation Network on the generated image x_i . The L_{gen} of the OrthoGAN is 0.25, which is lower than 0.27 L_{gen} of the TSynNet. This outcome represents the higher fineness of our model.

To evaluate the generation quality of the three models on teeth alignment, 30 patients were collected to validate the simulation results of the three models. The images were evaluated in three aspects including simulation authenticity, simulation aesthetics, image quality. The results were evaluated in a blind method by five doctors and five patients. The score ranges from 0 to 10 from low to high. In order to avoid subjective bias among different doctors and patients, we regard the average score of several patients as the final evaluation result.

The final data were shown as means (with standard deviations). Groups were compared by one -way analysis of variance, and the significance of mean difference within (intra) and between (inter) groups was performed using PSD post hoc test after ascertaining normality by the Shapiro-Wilk test and the homogeneity of variance between groups by the Levene test. A two-tailed P value less than 0.05 ($P < 0.05$) was considered to be statistically significant. All analyses were performed using SPSS software (Windows version 28.0; SPSS Inc., Chicago, IILL, USA).

The evaluation results of the doctors were shown in Table 1. The scores of simulation authenticity in OrthoGAN is statistically higher than that of TSynNet and pSp. The simulation aesthetics and image quality of OrthoGAN and TSynNet shows no difference, but is statistically higher than that of the pSp. In conclusion, the OrthoGAN shows the best performance in the view of orthodontics.

The evaluation results of the patients were shown in Table 1. OrthoGAN and TSynNet shows no difference in simulation authenticity, simulation aesthetics and image quality. The scores of OrthoGAN and TSynNet were higher than pSp, which indicates that pSp shows the worst performance in the eyes of doctors and patients.

According to the results of the clinical validation, we believe that the OrthoGAN model has made great progress in simulating the smiling results. Our results show that the simulation effect of OrthoGAN model is better than that of previous models, and it can meet the requirements of doctors more. The scores of clinical experiments shows the effectiveness and advantages of our approach in predicting the treatment effect in digital orthodontics.

4 Discussion

In this study, an image was generated based on the before-treatment frontal face image and the after-orthodontics 3D teeth model. We transfer the input modalities for the quality and efficiency of image generation. In the modal transfer stage, our differentiable rendering is more efficient and precise. During the experiment, we found that the EM algorithm in previous work relied heavily on the sampling of the initial landmarks. To reduce the uncertainty, previous work

firstly detect the position of the incisors and then sample the landmarks on the contour of incisors. The detection process undoubtedly consumes resources and brings new uncertainty: some patients whose smile faces do not have the clear incisor contour. Our method does not rely on any preconditions and its optimized parameters are explainable. The gradient descent which has been proved to be one of the most powerful optimizing method [26] accelerates our rendering process and make it a lot faster than the EM algorithm in previous work.

Hue is the general tendency of the color of the picture in a painting, and the hue of an image affects the overall color effect of the image. In the post-process stage of our approach, the resulting image is made to resemble the identity of the original person by changing the tone of the resulting teeth image to match the original teeth image, which is more natural and beautiful. we have to admit that even with more precise hue, the mouth image generated by pSp is more beautiful than OrthoGAN’s. However, according to the First Principle, pSp totally violate the shape of the 3D teeth model and can not be regarded as a qualified conditional teeth generation model. Actually, we intentionally take the pSp into our comparison to exhibit the style-based generation mechanism. The TSynNet which takes UNet architecture achieve to generated teeth with correct shape indeed. While the experiment shows that the TSynNet can not generate teeth as realistic as pSp, to improve this situation, our network takes both the style-based generation mechanism and the hierarchical feature extraction architecture of UNet (Figure 2(b)). Thus, the facial appearance and the corner shadow of our generated teeth images can be quite natural and have the exact same relative arrangement as the 3D teeth model indicated in the meantime. With the appropriate network structure design, we can take advantage of these two architectures for generating great mouth images which satisfy both the patients and orthodontists.

In addition, the entangled and confused input modalities of TSynNet lead to some obvious defects in the generated teeth image. Rather than directly providing TSynNet the label of the mouth like OrthoGAN, the iOrthoPredict cuts the teeth region of the mouth image according to the mouth label g_l and casts it to the TSynNet. This process forces the network to learn the outline of mouth region and the appearance of teeth from a single RGB image modality. However, even if the network is powerful enough to capture these features simultaneously, the geometry of the before-orthodontics teeth in the modality inevitably influence the training of TSynNet and make the edge of generated teeth blur (Figure 3). As for teeth geometry, our OrthoGAN takes the silhouettes of teeth and the teeth mask transferred by the depth image as input. The lack of the mask modality g_m in iOrthoPredictor makes the TSynNet less confident to generate the large teeth surface area compared with the sparse edge information and eventually causes the black spot on the face of the teeth (Figure 3). Without the occlusion of lips, our rendered teeth depth images and silhouettes contain the whole part of every tooth like Figure 1(f). To keep align with the silhouettes and masks extracted by segmentation networks like Figure 1(d) and 1(e), we cover the part of rendered g_s and g_m outside of g_l .

In Figure 4(a), we can observe that the frontal face images generated by pSp show clear inconsistent on the concatenated edge. The strategy introduced in Equal 4 help us circumvent this flaw while we can still make use of style-based architecture to simulate the complicated illumination effect.

There are still some limitations of our approach. Our method only focuses on the mouth region, thus the facial growth that could alter during the orthodontic treatment is untouched. Simulation based methods [27] may be exploited to solve this issue by taking facial bones into consideration.

5 Conclusion

On this basis, we conclude that this study proposed a high-precision visualization system for orthodontic smile simulation, which is based on deep learning. The system uses a series of image-based facial editing techniques to generate the most natural and accurate simulation results for users to date. Experiments and perceptual user studies on different settings shows the effectiveness of the our approach in predicting the treatment effect in digital orthodontics.

With the rapid development of image generation, our work focus on a feasible solution to a specific problem of orthodontic alignment, which is not well explored in the graphics community. It convincingly reveals that deep learning and artificial intelligence possess a great potential to develop more intelligent and efficient digital dental solutions. This may be considered a promising aspect of digital orthodontics and facial image manipulation.

6 Author Contributions

Feihong Shen, Youyi Zheng contributed to conception, design, data acquisition, analysis, and interpretation, drafted the manuscript, critically revised the manuscript; Jingjing Liu, contributed to data analysis and interpretation, critically revised the manuscript; Haizhen Li, contributed to data acquisition and interpretation, critically revised the manuscript; Fang Bing, contributed to data acquisition and interpretation, critically revised the manuscript; Chenglong Ma,

contributed to design and critically revised the manuscript; Feng Yang, Jin Hao, contributed to conception and critically revised the manuscript. All authors gave final approval and agree to be accountable for all aspects of the work.

7 Acknowledge

We strongly acknowledge the invaluable support of doctors and patients. The authors declare no potential conflicts of interest with respect to the author-ship and/or publication of this article.

References

- [1] Robert J Peterman, Shuying Jiang, Rene Johe, and Padma M Mukherjee. Accuracy of dolphin visual treatment objective (vto) prediction software on class iii patients treated with maxillary advancement and mandibular setback. *Progress in orthodontics*, 17(1):1–9, 2016.
- [2] G Power, J Breckon, M Sherriff, and F McDonald. Dolphin imaging software: an analysis of the accuracy of cephalometric digitization and orthognathic prediction. *International journal of oral and maxillofacial surgery*, 34(6):619–626, 2005.
- [3] Lingchen Yang, Zefeng Shi, Yiqian Wu, Xiang Li, Kun Zhou, Hongbo Fu, and Youyi Zheng. iorthopredictor: model-guided deep prediction of teeth alignment. *ACM Transactions on Graphics (TOG)*, 39(6):1–15, 2020.
- [4] Beijia Chen, Hongbo Fu, Kun Zhou, and Youyi Zheng. Orthoaligner: Image-based teeth alignment prediction via latent style manipulation. *IEEE Transactions on Visualization and Computer Graphics*, 2022.
- [5] Mehdi Mirza and Simon Osindero. Conditional generative adversarial nets. *arXiv preprint arXiv:1411.1784*, 2014.
- [6] Alec Radford, Luke Metz, and Soumith Chintala. Unsupervised representation learning with deep convolutional generative adversarial networks. *arXiv preprint arXiv:1511.06434*, 2015.
- [7] Andrew Brock, Jeff Donahue, and Karen Simonyan. Large scale gan training for high fidelity natural image synthesis. *arXiv preprint arXiv:1809.11096*, 2018.
- [8] Martin Arjovsky, Soumith Chintala, and Léon Bottou. Wasserstein generative adversarial networks. In *International conference on machine learning*, pages 214–223. PMLR, 2017.
- [9] Tero Karras, Samuli Laine, and Timo Aila. A style-based generator architecture for generative adversarial networks. In *Proceedings of the IEEE/CVF conference on computer vision and pattern recognition*, pages 4401–4410, 2019.
- [10] Huan Ling, Karsten Kreis, Daiqing Li, Seung Wook Kim, Antonio Torralba, and Sanja Fidler. Editgan: High-precision semantic image editing. *Advances in Neural Information Processing Systems*, 34:16331–16345, 2021.
- [11] Xun Huang, Arun Mallya, Ting-Chun Wang, and Ming-Yu Liu. Multimodal conditional image synthesis with product-of-experts gans. *ArXiv*, abs/2112.05130, 2021.
- [12] Olaf Ronneberger, Philipp Fischer, and Thomas Brox. U-net: Convolutional networks for biomedical image segmentation. In *International Conference on Medical image computing and computer-assisted intervention*, pages 234–241. Springer, 2015.
- [13] Zongwei Zhou, Md Mahfuzur Rahman Siddiquee, Nima Tajbakhsh, and Jianming Liang. Unet++: A nested u-net architecture for medical image segmentation. In *Deep learning in medical image analysis and multimodal learning for clinical decision support*, pages 3–11. Springer, 2018.
- [14] Özgün Çiçek, Ahmed Abdulkadir, Soeren S Lienkamp, Thomas Brox, and Olaf Ronneberger. 3d u-net: learning dense volumetric segmentation from sparse annotation. In *International conference on medical image computing and computer-assisted intervention*, pages 424–432. Springer, 2016.
- [15] Jieneng Chen, Yongyi Lu, Qihang Yu, Xiangde Luo, Ehsan Adeli, Yan Wang, Le Lu, Alan L Yuille, and Yuyin Zhou. Transunet: Transformers make strong encoders for medical image segmentation. *arXiv preprint arXiv:2102.04306*, 2021.
- [16] Elad Richardson, Yuval Alaluf, Or Patashnik, Yotam Nitzan, Yaniv Azar, Stav Shapiro, and Daniel Cohen-Or. Encoding in style: a stylegan encoder for image-to-image translation. In *Proceedings of the IEEE/CVF conference on computer vision and pattern recognition*, pages 2287–2296, 2021.
- [17] Xudong Mao, Liujuan Cao, Aurele T Gnanha, Zhenguo Yang, Qing Li, and Rongrong Ji. Cycle encoding of a stylegan encoder for improved reconstruction and editability. *arXiv preprint arXiv:2207.09367*, 2022.

- [18] Tengfei Wang, Yong Zhang, Yanbo Fan, Jue Wang, and Qifeng Chen. High-fidelity gan inversion for image attribute editing. In *Proceedings of the IEEE/CVF Conference on Computer Vision and Pattern Recognition*, pages 11379–11388, 2022.
- [19] Kaiming He, Xiangyu Zhang, Shaoqing Ren, and Jian Sun. Deep residual learning for image recognition. In *Proceedings of the IEEE conference on computer vision and pattern recognition*, pages 770–778, 2016.
- [20] Amit H Bermano, Rinon Gal, Yuval Alaluf, Ron Mokady, Yotam Nitzan, Omer Tov, Oren Patashnik, and Daniel Cohen-Or. State-of-the-art in the architecture, methods and applications of stylegan. In *Computer Graphics Forum*, volume 41, pages 591–611. Wiley Online Library, 2022.
- [21] Ian Goodfellow, Jean Pouget-Abadie, Mehdi Mirza, Bing Xu, David Warde-Farley, Sherjil Ozair, Aaron Courville, and Yoshua Bengio. Generative adversarial networks. *Communications of the ACM*, 63(11):139–144, 2020.
- [22] Andreas Lugmayr, Martin Danelljan, Andres Romero, Fisher Yu, Radu Timofte, and Luc Van Gool. Repaint: Inpainting using denoising diffusion probabilistic models. In *Proceedings of the IEEE/CVF Conference on Computer Vision and Pattern Recognition*, pages 11461–11471, 2022.
- [23] Erik Reinhard, Michael Adhikhmin, Bruce Gooch, and Peter Shirley. Color transfer between images. *IEEE Computer graphics and applications*, 21(5):34–41, 2001.
- [24] Daniel L Ruderman, Thomas W Cronin, and Chuan-Chin Chiao. Statistics of cone responses to natural images: implications for visual coding. *JOSA A*, 15(8):2036–2045, 1998.
- [25] Tero Karras, Samuli Laine, Miika Aittala, Janne Hellsten, Jaakko Lehtinen, and Timo Aila. Analyzing and improving the image quality of stylegan. In *Proceedings of the IEEE/CVF conference on computer vision and pattern recognition*, pages 8110–8119, 2020.
- [26] Sebastian Ruder. An overview of gradient descent optimization algorithms. *arXiv preprint arXiv:1609.04747*, 2016.
- [27] Rolf M. Koch, Markus Gross, Friedrich R. Carls, Daniel F. von Büren, George Fankhauser, and Yoav I. H. Parish. Simulating facial surgery using finite element models. *international conference on computer graphics and interactive techniques*, 1996.